SNHG5 knockdown alleviates neuropathic pain induced by chronic constriction injury via sponging miR-142-5p and regulating the expression of CAMK2A

SHENG JIN[*], SHIMING TIAN[*], HANLIN DING, ZHENGWEN YU and MINGQIANG LI

Department of Anesthesiology, Xiangyang Central Hospital, Affiliated Hospital of Hubei University of Arts and Science, Xiangyang, Hubei 441021, P.R. China

Abstract. Neuropathic pain (NP) is one of the most intractable diseases. The lack of effective therapeutic measures remains a major problem due to the poor understanding of the cause of NP. The aim of the present study was to investigate the effect of the long non-coding RNA small nucleolar RNA host gene 5 (SNHG5) in NP and the underlying molecular mechanism in order to identify possible therapeutic targets. A chronic constriction injury (CCI) mouse model was used to investigate whether SNHG5 prevents NP and the inflammatory response. Luciferase and RNA pull-down assays were used to detect the binding between SNHG5 and miR-142-5p as well as between miR-142-5p and CAMK2A. Western blot and qPCR were used to detect the RNA and protein expression. The results indicated that SNHG5 significantly inhibited CCI-induced NP. In addition, SNHG5 inhibited the inflammatory response through decreasing the release and the mRNA expression of interleukin (IL)-1β, IL-6, IL-10 and tumor necrosis factor-α. Mechanistically, SNHG5 acted via sponging microRNA-142-5p, thereby upregulating the expression of calcium/calmodulin-dependent protein kinase II α (CAMK2A). Further investigation indicated that CAMK2A knockdown also inhibited CCI-induced NP and inflammation. In summary, the present study demonstrated that SNHG5 silencing could alleviate the neuropathic pain induced by chronic constriction injury via sponging miR-142-5p and regulating the expression of CAMK2A.

Introduction

Neuropathic pain (NP), which is characterized by spontaneous pain, allodynia and hyperalgesia, is one of the most intractable diseases (1,2). NP may be caused by the dysfunction or primary injury of the somatosensory nervous system (3,4). NP adversely affects the quality of life of the patients and may lead to depression (5). Furthermore, the lack of satisfactory treatment and limited understanding of the underlying molecular mechanisms make NP one of the most serious health problems. Thus, it is crucial to explore the mechanisms underlying the occurrence and progression of NP.

Long non-coding RNAs (lncRNAs) are a class of non-coding RNAs that are >200 nucleotides in length and are involved in the regulation of several cellular processes (6,7), such as cell proliferation, apoptosis and differentiation, via regulating target gene expression (8). The lncRNA small nucleolar RNA host gene 5 (SNHG5) is a recently identified lncRNA that has yet to be extensively investigated, but has been found to be correlated with tumor range, metastasis, pathological stage and prognosis in various solid tumors (9). Moreover, SNHG5 has been indicated to play a key role in NP by sponging microRNA (miRNA/miR)-154-5p (10). However, the mechanism underlying the function of SNHG5 in the progression of NP is yet to be elucidated.

miRNAs/miRs are a group of single-stranded, non-coding RNAs that are 18-22 nucleotides in length (11) and play important roles in a variety of physiological and pathological processes, including cell proliferation and differentiation, apoptosis, metabolism and tumorigenesis (12) via negatively regulating the expression of their target genes (13). Numerous studies have indicated the critical role of miRs in the progression of NP (14).

The aim of the present study was to determine whether the expression of SNHG5 was dysregulated in chronic constriction

Correspondence to: Dr Hanlin Ding or Dr Zhengwen Yu, Department of Anesthesiology, Xiangyang Central Hospital, Affiliated Hospital of Hubei University of Arts and Science, 136 Jingzhou Street, Xiangcheng, Xiangyang, Hubei 441021, P.R. China
E-mail: dinghanlin1@yeah.net
E-mail: ojth75655@sina.cn

[*]Contributed equally

Abbreviations: CCI, chronic constriction injury; lncRNA, long non-coding RNA; IL, interleukin; miRs, microRNAs; NP, neuropathic pain; PWT, paw withdrawal threshold; PWTL, paw withdrawal threshold latency; SD, standard deviation; SNHG5, small nucleolar RNA host gene 5; TNF, tumor necrosis factor

injury (CCI) model mice. Functional studies were performed to evaluate the effect of SNHG5 on CCI-induced NP. Mechanistically, the interaction of SNHG5 with miR-142-5p and the downstream gene calcium/calmodulin-dependent protein kinase II α (CAMK2A) was investigated.

Materials and methods

Animals. A total of 48 female BALB/c mice (weight, 18-20 g; age, 5-6 weeks) were purchased from Beijing Vital River Laboratory Animal Technology Co., Ltd., and housed at 23℃ with a 12-h light/dark cycle under 40-50% humidity. The animals had access to food and water *ad libitum*. All animal experiments were approved by the Hubei University of Arts and Science (approval no. HUAS-A20191128; Xiangyang, China). This study was performed in accordance with the guidelines (15) for the Care and Use of Laboratory Animals. To evaluate the CCI model, 12 mice were randomly divided into the following two groups (n=6 per group): Sham and CCI model groups. To investigate SNHG5 function, 18 mice were randomly divided into the following three groups (n=6/group): Sham, CCI+adenovirus (Ad)-short hairpin (sh)RNA-negative control (NC) and CCI+Ad-sh-SNHG5 groups. To investigate the function of CAMK2A, 18 mice were randomly divided into the following three groups (n=6 per group): Sham, CCI+Ad-sh-NC and CCI+Ad-sh-CAMK2A groups.

CCI model establishment. After anesthesia with intraperitoneal injection of 1% sodium pentobarbital (50 mg/kg), an incision was made in the skin on the lateral surface of the thigh of the mice. The left common sciatic nerve was exposed at the mid-thigh level and was tightly ligated with a 5.0 silk suture at four sites along the nerve with a 1.0-1.5-mm distance between them. The muscle and skin were then sutured. The same procedures were performed in the mice of the sham group, but the sciatic nerve was left untied. At the end of the study, the mice were euthanized with an intraperitoneal injection of 3% sodium pentobarbital (160 mg/kg). When mice stopped breathing and the righting reflex disappeared, their death was verified and the dorsal root ganglia (DRG) were removed for further investigation.

Construction of adenovirus and administration. The 3rd generation of adenoviruses used to knock down SNHG5, CAMK2A and the negative control were prepared by RayBiotech, Inc. The shRNA and the whole sequence for SNHG5 along with their negative controls were synthetized. Recombinant adenoviruses ($1x10^8$ pfu, MOI=200:1) were injected using a microinjection syringe that was connected to the intrathecal catheter. Injections were performed 4 days before CCI surgery, and on days 0 and 7 after CCI surgery. The virus infection was performed 4 days before CCI operation because expression of SNHG5 started to reduce at day 4 after virus injection whereas the present study was investigating the effects of CCI treatment when SNHG5 expression was silenced.

Mechanical allodynia test. Mechanical allodynia was detected by measuring the paw withdrawal threshold (PWT) in response to a series of von Frey hair stimulations (Stoelting Co.). A series of von Frey filaments, starting with the filament 0.5 g, were applied to the dorsal surface of the hind paw with a sufficient force. PWT was defined as the pressure (g) at which the mouse withdrew its paw. The PWT was automatically recorded when the paw was withdrawn. Each trial was repeated six times at ~3-min intervals.

Thermal hyperalgesia test. Thermal hyperalgesia was detected by measuring paw withdrawal thermal latency (PWTL). Briefly, the plantar surface of the hind paw was irradiated using an infrared light beam generated by a modified Hargreaves device (Ugo Basile SRL). Subsequently, the PWTL (sec) was automatically recorded as soon as the mouse withdrew its paw.

RNA isolation and reverse transcription-quantitative PCR (RT-qPCR) analysis. Total RNA was extracted using TRIzol® reagent (Invitrogen; Thermo Fisher Scientific, Inc.), according to the manufacturer's instructions, and reverse-transcribed into cDNA using an EasyScript® First-Strand cDNA Synthesis SuperMix according to the manufacture's protocols (TransGen Biotech Co., Ltd.). qPCR was performed using SYBR Premix Ex Taq (Takara Biotechnology Co., Ltd.) on a Light Cycler® 480 System (Roche Diagnostics). qPCR was performed under the following thermocycling conditions: 95℃ for 30 sec, 40 cycles of 95℃ for 5 sec and 60℃ for 34 sec. mRNA GAPDH and U6 were used as the internal controls for mRNA or miRNA, respectively. The relative abundance of mRNA was calculated according to the $2^{-\Delta\Delta Cq}$ method (16). The qPCR primer sequences used were as follows: SNHG5 forward, 5'-TAC TGGCTGCGCACTTCG-3' and reverse, 5'-TACCCTGCA CAAACCCGAAA-3'; CAMK2A forward, 5'-TGACCTCAA CTACATGGTCTACA-3' and reverse, 5'-CTTCCCATTCTC GGCCTTG-3'; GAPDH forward, 5'-TATCCGCATCACTCA GTACCTG-3' and reverse, 5'-GAAGTGGACGATCTGCCA TTT-3'; miR-142-5p RT primer, GTCGTATCCAGTGCAGGG TCCGAGGTGCACTGGATACGACTCATCAC, forward, 5'-TGCGGGTATTTCATCTTTCGT-3' and reverse, 5'-CCA GTGCAGGGTCCGAGGT-3'; and U6 forward, 5'-CTCGCT TCGGCAGCACATATACT-3' and reverse, 5'-ACGCTTCAC GAATTTGCGTGTC-3'.

Western blot analysis. The L4-L6 spinal cord segments of each mouse were removed and treated with lysis buffer (Beyotime Institute of Biotechnology) containing protease inhibitor and phosphatase inhibitor cocktail (Sigma-Aldrich; Merck KGaA). BCA assay was used to detect the amount of protein. Proteins extracted from the spinal cord (40 μg) were separated via 10% SDS-PAGE followed by transfer onto PVDF membranes (EMD Millipore) and incubation with 5% non-fat dry milk in TBS containing 0.3% Tween-20 buffer for 2 h at room temperature. Subsequently, the blots were incubated with primary antibodies against CAMK2A (1:500, ab22609, Abcam) and GAPDH (1:1,000, ab245357, Abcam) at 4℃ for 12 h, followed by incubation with horseradish peroxidase-conjugated secondary antibody (1:1,000; cat. no. 6927-100, Amyjet) for another 2 h at room temperature. Finally, the blots were visualized using an enhanced chemiluminescence kit (Beyotime Institute of Biotechnology). The bands were semi-quantified using ImageJ software V1.8.0 (National Institutes of Health).

ELISA. All spinal cord samples were homogenized in RIPA lysis buffer (Beyotime Institute of Biotechnology) and, after centrifugation at 16,009.2 x g g at 4˚C for 15 min, the supernatants were collected. Total protein concentration was evaluated by a bicinchoninic acid assay protein assay kit (Thermo Fisher Scientific, Inc.). ELISA for tumor necrosis factor (TNF)-α (cat. no. 900-TM54), interleukin (IL)-6 (900-M50), IL-10 (900-T53) and IL-1β (900-K47) was performed following the manufacturer's protocol (PeproTech EC Ltd.).

Bioinformatics analysis. Bioinformatics website StarBase (starbase.sysu.edu.cn/) was used to predict the potential targets for SNHG5 and the target gene of miR-142-5p.

Cell transfection. 293 cells in the logic growth phase were transfected with miR-142-5p mimics (5'CATAAAGTAGTT TGCACTACT3'), mimic control (5'GTCAGTGGTCAAGTC AGTCAT3'), miR-142-5p inhibitor (5'AGTAGTGCAAAC TACTTTATG3'), inhibitor nc (5'CACGATTGAGATGAC CAGCAT'; all Genewiz, Suzhou, China), as well as pcDNA3.1 vector, pcDNA3.1/SNHG5, sh-nc (Top strand: CACCGTCCC AGGATTGTCAGCTGACCGAAGTCAGCTGACAATCCTGG GAC, Bottom strand: AAAAGTCCCAGGATTGTCAGCTGA CTTCGGTCAGCTGACAATCCTGGGAC) and sh-SNHG5 (Top strand: CACCGGGTTTGTGCAGGGTACAATGCG AACATTGTACCCTGCACAAACCC, Bottom strand: AAA AGGGTTTGTGCAGGGTACAATGTTCGCATTGTACCC TGCACAAACCC) using Lipofectamine® 2000 (Invitrogen; Thermo Fisher Scientific, Inc.) according to the manufacture's instructions at room temperature. Forty-eight hours after transfection, the cells can be used for the further experiments.

Dual-luciferase reporter assay. The wild-type (Wt) and mutant (Mut) SNHG5 or CAMK2A were obtained by chemical synthesis and subcloned into the pGL3 vector (Promega Corporation). Then, 293 cells obtained from American Type Culture Collection were co-transfected with the plasmid carrying Wt or Mut SNHG5/CAMK2A along with miR-142-5p mimics (5'CATAAAGTAGTTTGCACTACT3') or mimic control (5'GTCAGTGGTCAAGTCAGTCAT3') (Genewiz) using Lipofectamine® 2000 (Invitrogen; Thermo Fisher Scientific, Inc.). Subsequently, cells were transfected with 0.1 μg PRL-TK (TK-driven *Renilla* luciferase expression vector) as an internal control. Luciferase activities were measured 48 h after transfection with a dual-luciferase reporter assay kit (Promega Corporation).

RNA pull down assay. RNA pull down kit (cat. no. P0202, Geenseed) was used to perform RNA pull down assay. According to the manufacturer's instructions, after transfection for 48 h, the 293 cells were treated with cell lysate for 10 min. The cleavage was incubated with beads precoated with Streptavidin Magnetic Beads at 4˚C for 3 h. Then, the bound RNA was purified using Trizol regent (Boyetime) according to the protocols. The expression of LINC00917 or NLRP1 levels were measured by RT-qPCR as mentioned above.

Statistical analysis. All experiments were performed independently in triplicate. Data were analyzed using SPSS 17.0 (SPSS Inc.) and are presented as the mean ± standard deviation. Shapiro-Wilk test was used to detect normal distribution. Differences between two groups were determined using a unpaired Student's t-test or one-way ANOVA followed by Tukey's post hoc test. Pearson's correlation analysis was performed to analyze the correlation between miR-142-5p and SNHG5, miR-142-5p and CAMK2A and between SNHG5 and CAMK2A. $P<0.05$ was considered to indicate a statistically significant difference.

Results

SNHG5 is significantly upregulated in CCI mice. As shown in Fig. 1A-C, CCI decreased the PWT and the PWTL, whereas an increased number of paw lifts was observed after CCI surgery compared with the sham group, confirming that the CCI model was successfully established. Subsequently, the expression of SNHG5 was evaluated using RT-qPCR analysis. The results revealed that the expression of SNHG5 was significantly elevated in the DRG of the mice 7 days after CCI surgery, and reached the highest level at 15 days post-CCI surgery (Fig. 1D).

SNHG5 knockdown inhibits NP. As SNHG5 was found to be upregulated in mice with CCI-induced NP, whether SNHG5 plays a role in the regulation of NP was next investigated. Adenovirus vector was constructed to overexpress or silence the expression of SNHG5. RT-qPCR results indicated that the expression of SNHG5 was significantly upregulated in the SNHG5 overexpression group compared with the empty vector group, whereas SNHG5 expression was significantly inhibited in the sh-SNHG5 group compared with the sh-NC group (Fig. 2A). The mechanical allodynia test and thermal hyperalgesia test indicated that in the CCI+Ad-sh-SNHG5 group, PWT and the PWTL were increased, while the number of paw lifts was reduced compared with the CCI+Ad-sh-NC group (Fig. 2B-D). These results confirmed the critical role of SNHG5 in the development of NP.

SNHG5 knockdown inhibits the release and mRNA expression of IL-1β, IL-6 and TNF-α, but increases that of IL-10 induced by CCI. The levels of IL-1β, IL-6, IL-10 and TNF-α in DRG tissues and their mRNA expression were evaluated using ELISA and RT-qPCR analysis, respectively. The results revealed that the release and mRNA expression levels of IL-1β, IL-6 and TNF-α were significantly increased in the CCI+Ad-sh-NC group, while IL-10 was reduced in spinal cord tissue, compared with the sham group. Furthermore, in the CCI+Ad-sh-SNHG5 group, these increases in IL-1β, IL-6 and TNF-α expression levels were reversed, while the release and mRNA expression of IL-10 was significantly increased, compared with the CCI+Ad-sh-NC group (Fig. 3A and B).

SHNG5 sponges miR-142-5p. The bioinformatics website StarBase (http://starbase.sysu.edu.cn/) was used to predict the potential targets for SNHG5. As shown in Fig. 4A, binding sites for miR-142-5p were found within SNHG5. Subsequently, the dual-luciferase reporter assay confirmed that co-transfection of HEK-293 cells with Wt SMHG5 and miR-142-5p mimics resulted in significantly decreased luciferase activity
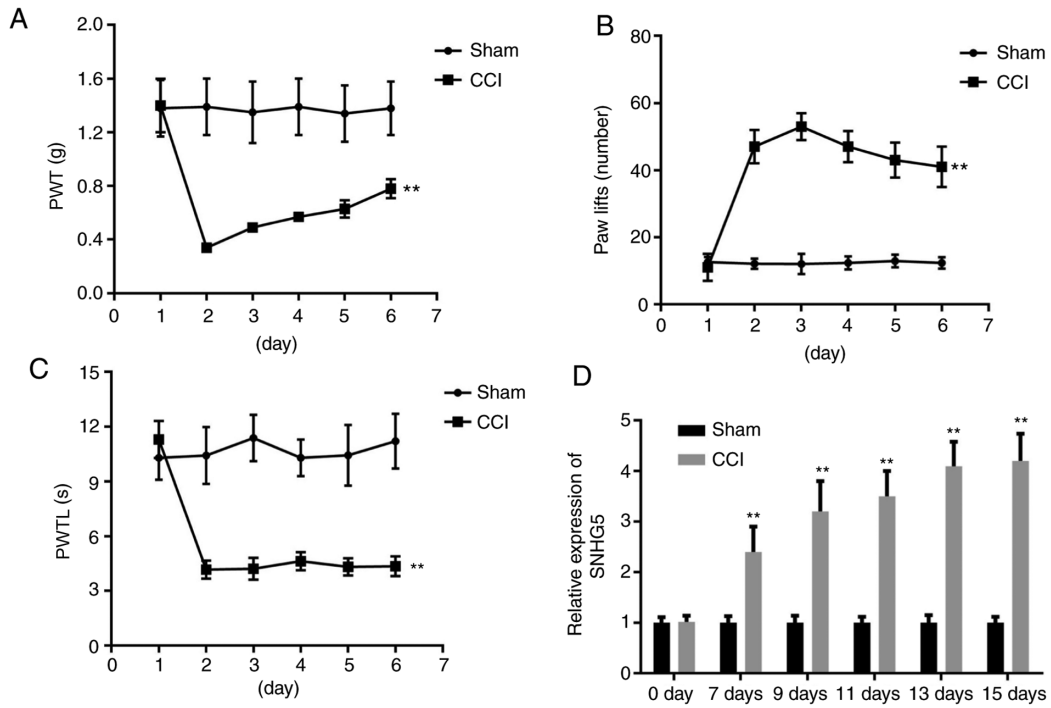
Figure 1. SNHG5 is upregulated in mice with neuropathic pain induced by CCI. (A) PWT was detected to evaluate mechanical allodynia (n=6). (B) The number of paw lifts was recorded to evaluate thermal allodynia (n=6). (C) PWTL was detected to evaluate thermal hyperalgesia (n=6). (D) Reverse transcription-quantitative PCR analysis was used to evaluate the expression of SNHG5 (n=6). $^{**}P<0.01$ vs. sham. CCI, chronic constriction injury; SNHG5, small nucleolar RNA host gene 5; PWT, paw withdrawal threshold; PWTL, paw withdrawal threshold latency.
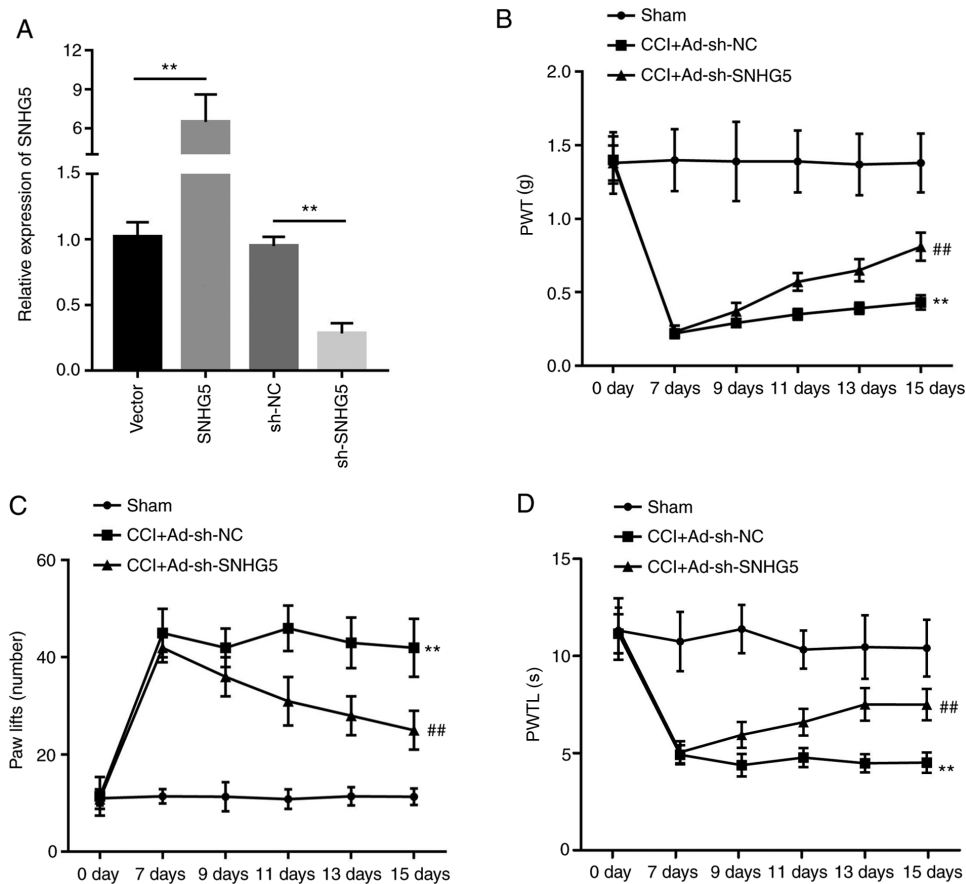

Figure 2. SNHG5 knockdown inhibits neuropathic pain induced by CCI. (A) Reverse transcription-quantitative PCR was used to evaluate the expression of SNHG5. $^{**}P<0.01$. (B) PWT was detected to evaluate mechanical allodynia (n=6). (C) The number of paw lifts was recorded to evaluate thermal allodynia (n=6). (D) PWTL was detected to evaluate thermal hyperalgesia (n=6). $^{**}P<0.01$ vs. sham; $^{##}P<0.01$ vs. CCI+Ad-sh-NC. CCI, chronic constriction injury; SNHG5, small nucleolar RNA host gene 5; PWT, paw withdrawal threshold; PWTL, paw withdrawal threshold latency; sh-, short hairpin RNA; NC, negative control; Ad-, adenovirus.
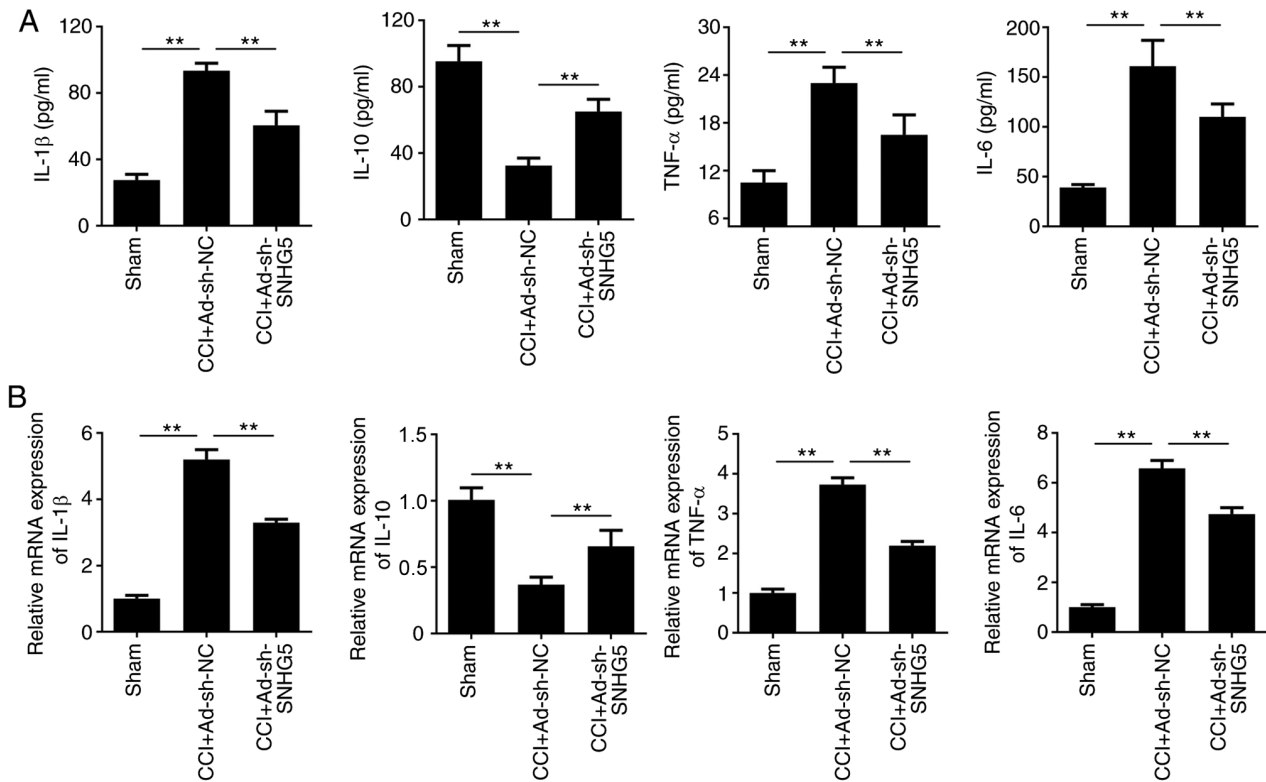
Figure 3. SNHG5 knockdown inhibits the release and mRNA expression of IL-1β, IL-6, IL-10 and TNF-α. (A) ELISA was used to evaluate the release of the inflammatory factors IL-1β, IL-6, IL-10 and TNF-α in the spinal cord (n=6). (B) Reverse transcription-quantitative PCR analysis was performed to evaluate the mRNA expression of IL-1β, IL-6, IL-10 and TNF-α in the spinal cord (n=6). **P<0.01. SNHG5, small nucleolar RNA host gene 5; IL-, interleukin; TNF, tumor necrosis factor; sh-, short hairpin RNA; NC, negative control; Ad-, adenovirus; CCI, chronic constriction injury.
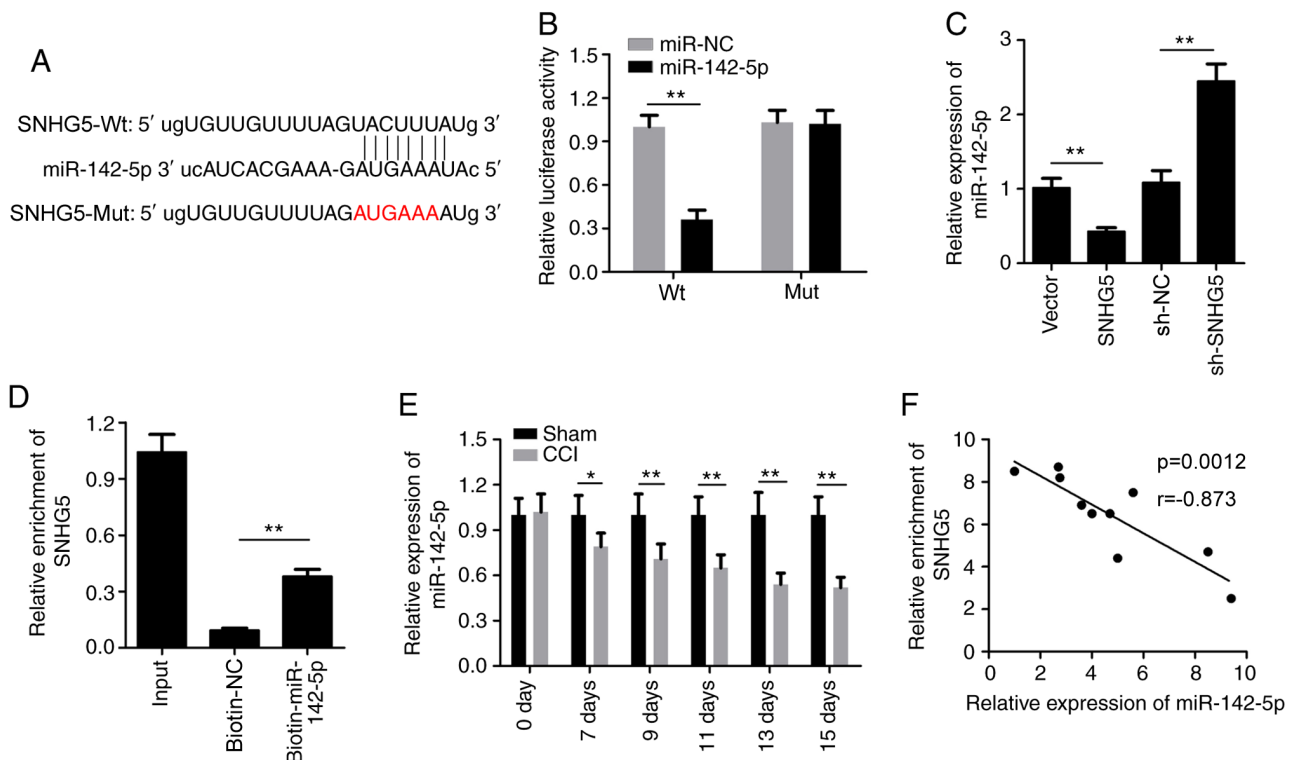

Figure 4. SNHG5 sponges miR-142-5p. (A) Bioinformatics analysis predicted the binding site between SNHG5 and miR-142-5p. (B) Dual-luciferase reporter assay was used to detect the interaction between SNHG5 and miR-142-5p (n=6). (C) RT-qPCR analysis was performed to evaluate the expression of miR-142-5p after SNHG5 silencing or overexpression (n=6). (D) RNA pull-down assay was used to detect the direct interaction between SNHG5 and miR-142-5p (n=3). (E) RT-qPCR analysis was performed to detect the expression of SNHG5 (n=6). (F) Pearson's correlation analysis was conducted to assess the correlation between SNHG5 and miR-142-5p. *P<0.05, **P<0.01. SNHG5, small nucleolar RNA host gene 5; miR, microRNA; RT-qPCR, reverse transcription-quantitative PCR; Wt, wild-type; Mut, mutant; NC, negative control; sh-, short hairpin RNA; CCI, chronic constriction injury.
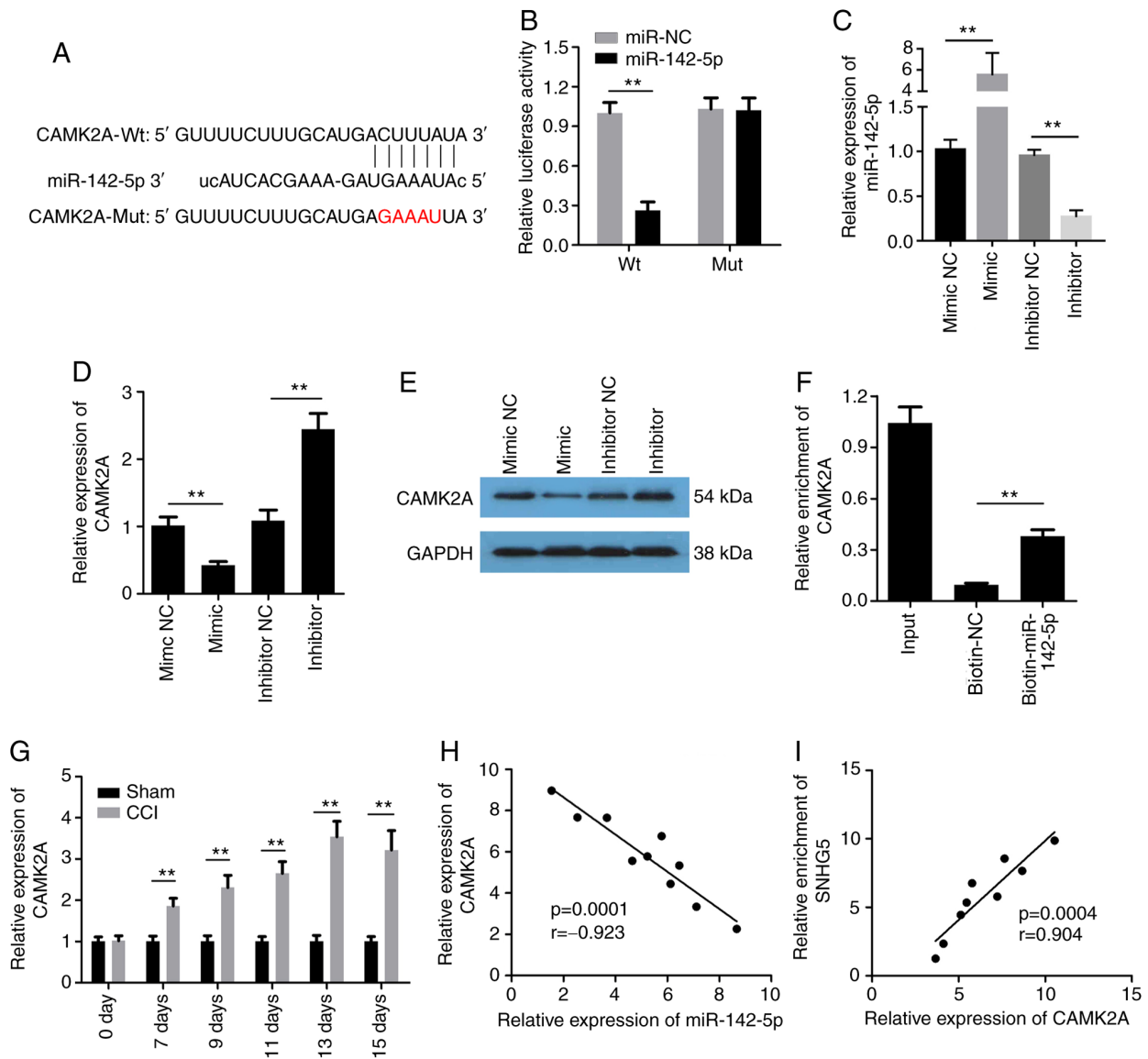
Figure 5. miR-142-5p directly targets CAMK2A. (A) Bioinformatics analysis predicted the binding cite between miR-142-5p and CAMK2A. (B) Dual-luciferase assay was used to detect the interaction between miR-142-5p and CAMK2A (n=6). (C-E) RT-qPCR analysis and western blotting were performed to evaluate the expression of miR-142 or CAMK2A (n=6). (F) RNA pull-down assay was used to detect the direct interaction between miR-142-5p and CAMK2A (n=3). (G) RT-qPCR analysis was performed to detect the expression of CAMK2A (n=6). (H and I) Pearson's correlation analysis was conducted to assess the correlation between miR-142-5p and CAMK2A, as well as between SNHG5 and CAMK2A. **$P<0.01$. CAMK2A, calcium/calmodulin-dependent protein kinase II α; miR, microRNA; SNHG5, small nucleolar RNA host gene 5; RT-qPCR, reverse transcription-quantitative PCR; Wt, wild-type; Mut, mutant; NC, negative control; sh-, short hairpin RNA; CCI, chronic constriction injury.

compared with the miR-NC group (Fig. 4B). In addition, the relative expression of miR-142-5p was significantly decreased in the SNHG5 overexpression group and increased in the sh-SNHG5 group (Fig. 4C). Then, the RNA pull-down assay verified that biotinylated-miR-142-5p, but not biotinylated-NC, could enrich SNHG5 (Fig. 4D). The results of the RT-qPCR analysis indicated that miR-142-5p expression was significantly downregulated after CCI (Fig. 4E). The Pearson's correlation analysis demonstrated that there was a negative correlation between miR-142-5p and SNHG5 (Fig. 4F).

miR-142-5p targets CAMK2A. It is well known that miRs bind to their target genes to inhibit their expression. Thus, the present study attempted to identify the target gene of miR-142-5p in order to elucidate its underlying mechanism

of action. The bioinformatics website StarBase was used to predict the potential targets of miR-142-5p. As shown in Fig. 5A, binding sites for miR-142-5p were found within CAMK2A. Subsequently, the dual-luciferase reporter assay confirmed that co-transfection of HEK-293 cells with Wt SAMK2A and the miR-142-5p mimics resulted in significantly decreased luciferase activity compared with the miR-NC group (Fig. 5B). miR-142-5p mimic significantly increased the expression of miR-142-5p, while miR-142-5p inhibitor reduced the expression of miR-142-5p (Fig. 5C). In addition, the relative expression of CAMK2A was significantly decreased in the miR-142-5p mimic group, and it increased in the miR-142-5p inhibitor group (Fig. 5D and E). Then, the RNA pull-down assay verified that biotinylated-miR-142-5p, but not biotinyl-ated-NC, could enrich CAMK2A (Fig. 5F). The results of the
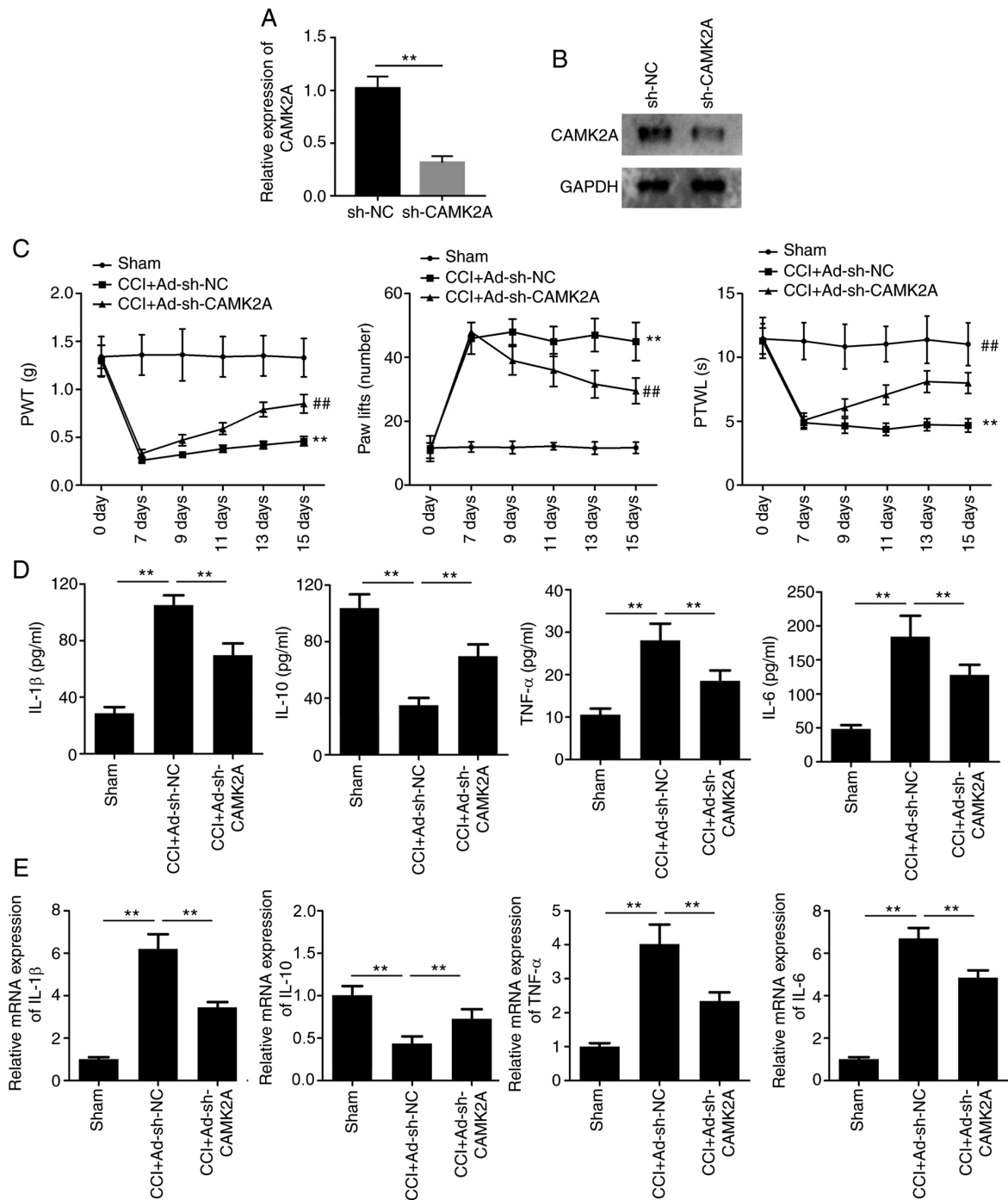
Figure 6. CAMK2A knockdown inhibits neuropathic pain and inflammatory response induced by CCI. (A) RT-qPCR and (B) western blotting was performed to detect the expression of CAMK2A. **P<0.01 vs. sh-NC. (C) PWT, number of paw lifts and PWTL were detected to evaluate mechanical allodynia, thermal allodynia and thermal hyperalgesia (n=6). (D) ELISA was used to evaluate the levels of inflammatory factors, including IL-1β, IL-6, IL-10 and TNF-α, in the spinal cord (n=6). (E) RT-qPCR analysis was performed to evaluate the mRNA expression of IL-1β, IL-6, IL-10 and TNF-α in the spinal cord (n=6). **P<0.01 vs. sham; $^{##}$P<0.01 vs. CCI+Ad-sh-NC. CCI, chronic constriction injury; CAMK2A, calcium/calmodulin dependent protein kinase II α; RT-qPCR, reverse transcription-quantitative PCR; NC, negative control; sh-, short hairpin RNA; PWT, paw withdrawal threshold; PWTL, paw withdrawal threshold latency; IL-, interleukin; TNF, tumor necrosis factor; Ad-, adenovirus.

RT-qPCR analysis indicated that CAMK2A was significantly upregulated after CCI (Fig. 5G). The Pearson's correlation analysis demonstrated that there was a strong negative correlation between miR-142-5p and CAMK2A (Fig. 5H) and a strong positive correlation between CAMK2A and SNHG5 (Fig. 5I).

CAMK2A knockdown inhibits NP and the inflammatory response induced by CCI. To further elucidate the role of

CAMK2A, adenovirus for silencing CAMK2A was established. RT-qPCR and western blot analysis indicated that transfection with sh-CAMK2A significantly reduced the expression of CAMK2A (Fig. 6A and B). The mechanical allodynia and thermal hyperalgesia tests indicated that PWT and PWTL were increased in the CCI+Ad-sh-CAMK2A group, while the number of paw lifts was reduced, compared with the CCI+Ad-sh-NC group (Fig. 6C). Furthermore, the levels of IL-1β, IL-6, IL-10

and TNF-α in DRG tissues and their mRNA expression were evaluated using ELISA and RT-qPCR analysis, respectively. The results revealed that in the CCI+Ad-sh-NC group, the release and mRNA expression levels of IL-1β, IL-6 and TNF-α were significantly increased, while IL-10 was reduced in spinal cord tissue, compared with in the sham group. Furthermore, in the CCI+Ad-sh-CAMK2A group, this increase in IL-1β, IL-6 and TNF-α was reversed, while the inhibition of the release and mRNA expression of IL-10 was markedly reversed, compared with the CCI+Ad-sh-NC group (Fig. 6D and E).

Discussion

The aim of the present study, was to explore the anti-nociceptive effect of the lncRNA SNHG5 on CCI-induced inflammatory response and NP. The results revealed that SNHG5 knockdown markedly inhibited mechanical and thermal hyperalgesia. Further investigation was undertaken to determine the effects of SNHG5 on the release of inflammatory factors, such as IL-1β, IL-6, TNF-α and IL-10. The results of the present study were consistent with previously reported findings (9). The majority of the studies of SNHG5 are in the field of human cancer, including gastric, breast, liver and esophageal cancer (17-21). In addition, SNHG5 has been reported to regulate cell apoptosis and the inflammatory response in chronic obstructive pulmonary disease via sponging miR-132 (22).

Mechanistically, the results of the current study indicated that SNHG5 can sponge miR-142-5p to upregulate the expression CAMK2A. SNHG5 has been demonstrated to be capable of sponging various miRs, such as miR-32, miR-212-3p, miR-26-5p, miR-154-5p, miR-23a and miR-26a (17,18,23-26). To the best of our knowledge, the present study was the first to reveal that SNHG5 interacts with miR-142-5p.

miR-142-5p has been investigated in the context of NP. It was reported that miR-142-3p could inhibit NP development via inhibiting HMGB1 expression (27). Adeno-associated virus vector overexpressing miR-142-5p was able to inhibit NP in rats through binding to the 3'-untranslated region of the mRNA and inhibiting its expression (28). In the present study, it was also observed that miR-142-5p was downregulated in CCI rats, which was consistent with these previous findings. Although, the direct effect of miR-142-5p on CCI was not evaluated, which is a limitation of the present study. As it is known that miRs bind to their target mRNAs to inhibit their expression, we attempted to identify the target gene of miR-142-5p. Finally, CAMK2A was predicted and verified to be the target of miR-142-5p.

CAMK2A is a serine/threonine protein kinase, which can be found in sensory axons and is involved in neuroplasticity (29-32). It was previously demonstrated that CAMK2A silencing can inhibit complete Freund's adjuvant-induced NP (33). Ryanodine receptors, which is capable of producing a focal high concentration of calcium and is found in close proximity to CAMK2A, activates CAMK2A to produce hyperalgesic priming (34). Furthermore, CAMK2A knockdown was also found to suppress NP induced by spinal nerve ligation (35). In addition, it was reported that CAMK2A plays a key role during the transition from acute to chronic pain (35). These findings indicated that CAMK2A may be intricately involved in the regulation of NP. Of note, a selective inhibitor of CAMK2A, KN93, has been developed, and it can reduce

both mechanical and thermal hypersensitivity (36). The present study further confirmed that CAMK2A was upregulated in CCI-induced NP and that silencing of CAMK2A could alleviate the pain induced by CCI.

The downstream genes regulated by CAMK2A were not investigated in the present study. CAMK2A was previously reported to regulate the function of the cytoplasmic polyadenylation element-binding protein by phosphorylating the regulatory site threonine 171 (37). Activated CAMK2A can phosphorylate the N-methyl-D-aspartate receptor and promote its activation (38). The downstream gene(s) modulated by CAMK2A will be investigated in future studies.

In the present study, we did not investigate the direct effect of miR-142-5p to support the conclusions, and more studies are required to fully elucidate the interaction between miR-142-5p and CAMK2A. Rescue experiments should be performed to further confirm the interaction between SNHG5 and miR-142-5p, as well as between miR-142-5p and CAMK2A. These limitations will be studied in our further research.

Coronavirus disease 2019 has affected tens of millions of individuals globally. At present, the mRNA vaccine BNT162b2 has been used for the prevention of this epidemic (39). In the future, more therapeutic methods based on RNA will likely be utilized. With further investigation of the effects and underlying mechanisms of the SNHG5/miR-142-5p/CAMK2A signaling pathway, these molecules could be used as a therapeutic or diagnostic target for NP. However, further studies are required before any issues with stability, efficacy and side effects are solved.

In conclusion, the present study demonstrated that the effects of the lncRNA SNHG5 on CCI-induced NP are mediated through regulation of the miR-142-5p/CAMK2A signaling pathway. These findings may improve our understanding of the mechanism underlying the function of SNHG5 in NP.

Availability of data and materials

The datasets generated and/or analyzed during the current study are available from the corresponding author on reasonable request.

Authors' contributions

HD and ZY designed this study. SJ, ST and ML performed all the experiments. ML was responsible for data analysis. SJ and ST drafted the manuscript. SJ, ST, HD and ZY revised the paper. SJ, ST and ZY confirm the authenticity of all the raw data. All authors read and approved the final manuscript.

Ethics approval and consent to participate

This study was approved by the Hubei University of Arts and Science (Xiangyang, China) and were performed in

accordance with the Guidelines for the Care and Use of Laboratory Animals.

Patient consent for publication

Not applicable.

Competing interests

The authors declare that they have no competing interests.

References

1. Costigan M, Scholz J and Woolf CJ: Neuropathic pain: A maladaptive response of the nervous system to damage. Annu Rev Neurosci 32: 1-32, 2009.
2. Calvo M, Davies AJ, Hébert HL, Weir GA, Chesler EJ, Finnerup NB, Levitt RC, Smith BH, Neely GG, Costigan M and Bennett DL: The genetics of neuropathic pain from model organisms to clinical application. Neuron 104: 637-653, 2019.
3. Campbell JN and Meyer RA: Mechanisms of neuropathic pain. Neuron 52: 77-92, 2006.
4. Tramullas M, Francés R, de la Fuente R, Velategui S, Carcelén M, García R, Llorca J and Hurlé MA: MicroRNA-30c-5p modulates neuropathic pain in rodents. Sci Transl Med 10: eaao6299, 2018.
5. Descalzi G, Mitsi V, Purushothaman I, Gaspari S, Avrampou K, Loh YHE, Shen L and Zachariou V: Neuropathic pain promotes adaptive changes in gene expression in brain networks involved in stress and depression. Sci Signal 471: eaaj1549, 2017.
6. Yao RW, Wang Y and Chen LL: Cellular functions of long noncoding RNAs. Net Cell Biol 21: 542-551, 2019.
7. Boon RA, Jaé N, Holdt L and Dimmeler S: Long noncoding RNAs: From clinical genetics to therapeutic targets? J Am Coll Cardiol 67: 1214-1226, 2016.
8. Long Y, Wang X, Youmans DT and Cech TR: How do lncRNAs regulate transcription? Sci Adv 3: eaao2110, 2017.
9. Han W, Shi J, Cao J, Dong B and Guan W: Latest advances of long non-coding RNA SNHG5 in human cancers. Onco Targets Ther 13: 6393-6403, 2020.
10. Chen M, Yang Y, Zhang W, Li X, Wu J, Zou X and Zeng X: Long noncoding RNA SNHG5 knockdown alleviates neuropathic pain by targeting the miR-154-5p/CXCL13 axis. Neurochem Res 45: 1566-1575, 2020.
11. Shang Q, Yang Z, Jia R and Ge S: The novel roles of circRNAs in human cancer. Mol Cancer 18: 6, 2019.
12. Huang T, Wan X, Alvarez AA, James CD, Song X, Yang Y, Sastry N, Nakano I, Sulman EP, Hu B and Cheng SY: MIR93 (microRNA-93) regulates tumorigenicity and therapy response of glioblastoma by targeting autophagy. Autophagy 15: 1100-1111, 2019.
13. Bhaskaran V, Yao Y, Bei F and Peruzzi P: Engineering, delivery, and biological validation of artificial microRNA clusters for gene therapy applications. Nat Protoc 14: 3538-3553, 2019.
14. Yang Y, Ding L, Hu Q, Xia J, Sun J, Wang X, Xiong H, Gurbani D, Li L, Liu Y and Liu A: MicroRNA-218 functions as a tumor suppressor in lung cancer by targeting IL-6/STAT3 and negatively correlates with poor prognosis. Mol Cancer 16: 141, 2017.
15. Sun D, Yue B, Sun R, Wang T, Pang W, Kong Q, Zhu D, Li N and Qin C: Laboratory animal-Guideline for ethical review of animal welfare (GBT35892-2018), China. 2018. https://www.chinesestandard.net/PDF.aspx/GBT35892-2018. Accessed February 6, 2018.
16. Zhao L, Han T, Li Y, Sun J, Zhang S, Liu Y, Shan B, Zheng D and Shi J: The lncRNA SNHG5/miR-32 axis regulates gastric cancer cell proliferation and migration by targeting KLF4. Faseb J 31: 893-903, 2017.
17. Livak KJ and Schmittgen TD: Analysis of relative gene expression data using real-time quantitative PCR and the 2(-Delta Delta C(T)) method. Methods 25: 402-408, 2001.
18. Chi JR, Yu ZH, Liu BW, Zhang D, Ge J, Yu Y and Cao XC: SNHG5 promotes breast cancer proliferation by sponging the miR-154-5p/PCNA axis. Mol Ther Nucleic Acids 17: 138-149, 2019.
19. Li Y, Guo D, Zhao Y, Ren M, Lu G, Wang Y, Zhang J, Mi C, He S and Lu X: Long non-coding RNA SNHG5 promotes human hepatocellular carcinoma progression by regulating miR-26a-5p/GSK3β signal pathway. Cell Death Dis 9: 888, 2018.
20. Wang QY, Peng L, Chen Y, Liao LD, Chen JX, Li M, Li YY, Qian FC, Zhang YX, Wang F, et al: Characterization of super-enhancer-associated functional lncRNAs acting as ceRNAs in ESCC. Mol Oncol 14: 2203-2230, 2020.
21. Zhao L, Guo H, Zhou B, Feng J, Li Y, Han T, Liu L, Li L, Zhang S, Liu Y, et al: Long non-coding RNA SNHG5 suppresses gastric cancer progression by trapping MTA2 in the cytosol. Oncogene 35: 5770-5780, 2016.
22. Shen Q, Zheng J, Wang X, Hu W, Jiang Y and Jiang Y: lncRNA SNHG5 regulates cell apoptosis and inflammation by miR-132/PTEN axis in COPD. Biomed Pharmacother 126: 110016, 2020.
23. Ju C, Zhou R, Sun J, Zhang F, Tang X, Chen KK, Zhao J, Lan X, Lin S, Zhang Z and Lv XB: lncRNA SNHG5 promotes the progression of osteosarcoma by sponging the miR-212-3p/SGK3 axis. Cancer Cell Int 18: 141, 2018.
24. Gao J, Zeng K, Liu Y, Gao L and Liu L: lncRNA SNHG5 promotes growth and invasion in melanoma by regulating the miR-26a-5p/TRPC3 pathway. Onco Targets Ther 12: 169-179, 2019.
25. Lin H, Shen L, Lin Q, Dong C, Maswela B, Illahi GS and Wu X: SNHG5 enhances Paclitaxel sensitivity of ovarian cancer cells through sponging miR-23a. Biomed Pharmacother 123: 109711, 2020.
26. Wang Z, Wang Z, Liu J and Yang H: Long non-coding RNA SNHG5 sponges miR-26a to promote the tumorigenesis of osteosarcoma by targeting ROCK1. Biomed Pharmacother 107: 598-605, 2018.
27. Zhang Y, Mou J, Cao L, Zhen S, Huang H and Bao H: MicroRNA-142-3p relieves neuropathic pain by targeting high mobility group box 1. Int J Mol Med 41: 501-510, 2018.
28. Xu H, Yue C and Chen L: Post-transcriptional regulation of soluble guanylate cyclase that governs neuropathic pain in Alzheimer's disease. J Alzheimers Dis 71: 1331-1338, 2019.
29. Giese KP, Fedorov NB, Filipkowski RK and Silva AJ: Autophosphorylation at Thr286 of the alpha calcium-calmodulin kinase II in LTP and learning. Science 279: 870-873, 1998.
30. Gleason MR, Higashijima S, Dallman J, Liu K, Mandel G and Fetcho JR: Translocation of CaM kinase II to synaptic sites in vivo. Nat Neurosci 6: 217-218, 2003.
31. Geddis MS and Rehder V: The phosphorylation state of neuronal processes determines growth cone formation after neuronal injury. J Neurosci Res 74: 210-220, 2003.
32. VanBerkum MF and Goodman CS: Targeted disruption of Ca(2+)-calmodulin signaling in Drosophila growth cones leads to stalls in axon extension and errors in axon guidance. Neuron 14: 43-56, 1995.
33. Luo F, Yang C, Chen Y, Shukla P, Tang L, Wang LX and Wang ZJ: Reversal of chronic inflammatory pain by acute inhibition of Ca2+/calmodulin-dependent protein kinase II. J Pharmacol Exp Ther 325: 267-275, 2008.
34. Chen Y, Luo F, Yang C, Kirkmire CM and Wang ZJ: Acute inhibition of Ca2+/calmodulin-dependent protein kinase II reverses experimental neuropathic pain in mice. J Pharmacol Exp Ther 330: 650-659, 2009.
35. Ferrari LF, Bogen O and Levine JD: Role of nociceptor αCaMKII in transition from acute to chronic pain (hyperalgesic priming) in male and female rats. J Neurosci 33: 11002-11011, 2013.
36. He Y, Chen Y, Tian X, Yang C, Lu J, Xiao C, DeSimone J, Wilkie DJ, Molokie RE and Wang ZJ: CaMKIIα underlies spontaneous and evoked pain behaviors in Berkeley sickle cell transgenic mice. Pain 157: 2798-2806, 2016.
37. Atkins CM, Nozaki N, Shigeri Y and Soderling TR: Cytoplasmic polyadenylation element binding protein-dependent protein synthesis is regulated by calcium/calmodulin-dependent protein kinase II. J Neurosci 24: 5193-5201, 2004.
38. Kitamura Y, Miyazaki A, Yamanaka Y and Nomura Y: Stimulatory effects of protein kinase C and calmodulin kinase II on N-methyl-D-aspartate receptor/channels in the postsynaptic density of rat brain. J Neurochem 61: 100-109, 1993.
39. Tartof SY, Slezak JM, Fischer H, Hong V, Ackerson BK, Ranasinghe ON, Frankland TB, Ogun OA, Zamparo JM, Gray S, et al: Effectiveness of mRNA BNT162b2 COVID-19 vaccine up to 6 months in a large integrated health system in the USA: A retrospective cohort study. Lancet 398: 1407-1416, 2021.